LETTER

doi:10.1038/nature14241

An ultraluminous quasar with a twelve-billion-solar-mass black hole at redshift 6.30

Xue-Bing Wu[1,2], Feige Wang[1,2], Xiaohui Fan[2,3], Weimin Yi[4,5,6], Wenwen Zuo[7], Fuyan Bian[8], Linhua Jiang[2], Ian D. McGreer[3], Ran Wang[2], Jinyi Yang[1,2], Qian Yang[1,2], David Thompson[9] & Yuri Beletsky[10]

So far, roughly 40 quasars with redshifts greater than $z = 6$ have been discovered[1–8]. Each quasar contains a black hole with a mass of about one billion solar masses ($10^9\ M_\odot$)[2,6,7,9–13]. The existence of such black holes when the Universe was less than one billion years old presents substantial challenges to theories of the formation and growth of black holes and the coevolution of black holes and galaxies[14]. Here we report the discovery of an ultraluminous quasar, SDSS J010013.02+280225.8, at redshift $z = 6.30$. It has an optical and near-infrared luminosity a few times greater than those of previously known $z > 6$ quasars. On the basis of the deep absorption trough[15] on the blue side of the Lyman-α emission line in the spectrum, we estimate the proper size of the ionized proximity zone associated with the quasar to be about 26 million light years, larger than found with other $z > 6.1$ quasars with lower luminosities[16]. We estimate (on the basis of a near-infrared spectrum) that the black hole has a mass of $\sim 1.2 \times 10^{10}\ M_\odot$, which is consistent with the $1.3 \times 10^{10}\ M_\odot$ derived by assuming an Eddington-limited accretion rate.

High-redshift quasars have been efficiently selected using a combination of optical and near-infrared colours[3,4]. We have carried out a systematic survey of quasars at $z > 5$ using photometry from the Sloan Digital Sky Survey (SDSS)[17], the two Micron All Sky Survey (2MASS)[18] and the Wide-field Infrared Survey Explorer (WISE)[19], resulting in the discovery of a significant population of luminous high-redshift quasars. SDSS J010013.02+280225.8 (hereafter J0100+2802) was selected as a high-redshift quasar candidate owing to its red optical colour (with SDSS AB magnitudes $i_{AB} = 20.84 \pm 0.06$ and $z_{AB} = 18.33 \pm 0.03$) and a photometric redshift of $z \approx 6.3$. It has bright detections in the 2MASS J, H and K_s bands with Vega magnitudes of 17.00 ± 0.20, 15.98 ± 0.19 and 15.20 ± 0.16, respectively; it is also strongly detected in WISE, with Vega magnitudes in W1 to W4 bands of 14.45 ± 0.03, 13.63 ± 0.03, 11.71 ± 0.21 and 8.98 ± 0.44, respectively (see Extended Data Figs 1 and 2 for images in different bands). Its colour in the two bluest WISE bands, W1 and W2, clearly differentiates it from the bulk of stars in our Galaxy[20]. The object was within the SDSS-III imaging area. It is close to the colour selection boundary of SDSS $z \approx 6$ quasars[1], but was assigned to low priority earlier because of its relatively red $z_{AB} - J$ colour and its bright apparent magnitudes. It is undetected in both radio and X-ray bands by the wide-area, shallow survey instruments.

Initial optical spectroscopy on J0100+2802 was carried out on 29 December 2013 with the Lijiang 2.4-m telescope in China. The low-resolution spectrum clearly shows a sharp break at about 8,800 Å, consistent with a quasar at a redshift beyond 6.2. Two subsequent optical spectroscopic observations were conducted on 9 and 24 January 2014 respectively with the 6.5-m Multiple Mirror Telescope (MMT) and the twin 8.4-m mirror Large Binocular Telescope (LBT) in the USA. The Lyman-α (Lyα) line shown in the spectra confirms that J0100+2802 is a quasar at a redshift of 6.30 ± 0.01 (see Fig. 1 and Methods for details).

We use the multiwavelength photometry to estimate the optical luminosity at rest-frame wavelength 3,000 Å ($L_{3,000}$), which is consistent with that obtained from K-band spectroscopy (see below). The latter gives a more reliable value of $(3.15 \pm 0.47) \times 10^{47}$ erg s^{-1}, adopting a ΛCDM cosmology with Hubble constant $H_0 = 70$ km s^{-1} Mpc^{-1}, matter density parameter $\Omega_M = 0.30$ and dark energy density parameter $\Omega_\Lambda = 0.7$. Assuming an empirical conversion factor from the luminosity at 3,000 Å to the bolometric luminosity[21], this gives $L_{bol} = 5.15 \times L_{3,000} = 1.62 \times 10^{48}$ erg s^{-1} $= 4.29 \times 10^{14}\ L_\odot$ (where $L_\odot$ is the solar luminosity). We obtain a similar result when estimating the bolometric luminosity from the Galactic extinction corrected absolute magnitude at rest-frame 1,450 Å, which is $M_{1450,AB} = -29.26 \pm 0.20$. The luminosity of this

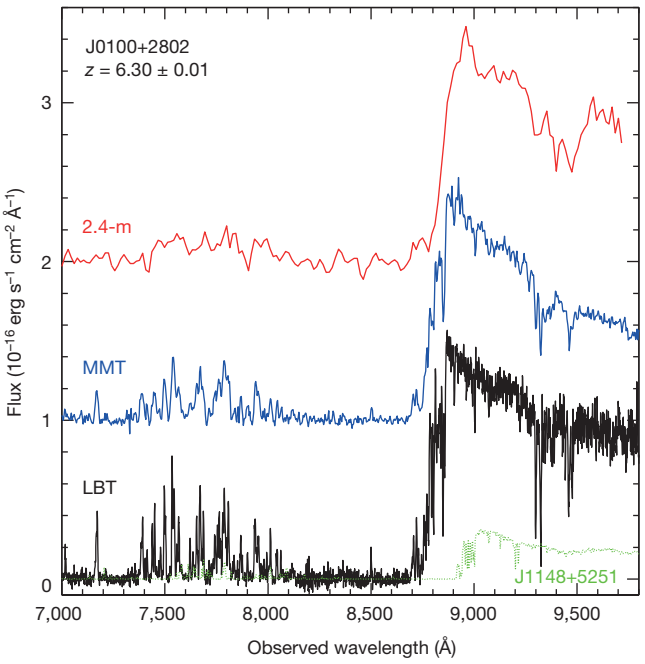

Figure 1 | The optical spectra of J0100+2802. From top to bottom, spectra taken with the Lijiang 2.4-m telescope, the MMT and the LBT (in red, blue and black colours), respectively. For clarity, two spectra are offset upward by one and two vertical units. Although the spectral resolution varies from very low to medium, in all spectra the Lyα emission line, with a rest-frame wavelength of 1,216 Å, is redshifted to around 8,900 Å, giving a redshift of 6.30. J0100+2802 is a weak-line quasar with continuum luminosity about four times higher than that of SDSS J1148+5251 (in green on the same flux scale)[1], which was previously the most luminous high-redshift quasar known at $z = 6.42$.

[1]Department of Astronomy, School of Physics, Peking University, Beijing 100871, China. [2]Kavli Institute for Astronomy and Astrophysics, Peking University, Beijing 100871, China. [3]Steward Observatory, University of Arizona, Tucson, Arizona 85721-0065, USA. [4]Yunnan Observatories, Chinese Academy of Sciences, Kunming 650011, China. [5]University of Chinese Academy of Sciences, Beijing 100049, China. [6]Key Laboratory for the Structure and Evolution of Celestial Objects, Chinese Academy of Sciences, Kunming 650011, China. [7]Shanghai Astronomical Observatory, Chinese Academy of Sciences, Shanghai 200030, China. [8]Mount Stromlo Observatory, Research School of Astronomy and Astrophysics, Australian National University, Weston Creek, Australian Capital Territory 2611, Australia. [9]Large Binocular Telescope Observatory, University of Arizona, Tucson, Arizona 85721, USA. [10]Las Campanas Observatory, Carnegie Institution of Washington, Colina el Pino, Casilla 601, La Serena, Chile.

quasar is roughly 4 times greater than that of the luminous $z = 6.42$ quasar[1] SDSS J1148+5251, and 7 times greater than that of the most distant known quasar[6] ULAS J1120+0641 ($z = 7.085$); it is the most luminous quasar known at $z > 6$ (see Extended Data Fig. 3).

The rest-frame equivalent width of the Lyα + N v emission lines as measured from the LBT spectrum is roughly 10 Å, suggesting that J0100+2802 is probably a weak-line quasar (WLQ)[22]. The fraction of WLQs is higher among the $z \approx 6$ quasars compared to those at lower redshift[8], and a high detection rate of strong millimetre dust continuum in $z \approx 6$ WLQs points to active star formation in these objects[23]. Given its extreme luminosity, J0100+2802 will be helpful in the study of the evolutionary stage of WLQs by future (sub)millimetre observations, though the origin of the weak ultraviolet emission line feature of WLQs is still uncertain.

The LBT spectrum of J0100+2802 (Fig. 1) exhibits a deep Gunn–Peterson absorption trough[15] blueward of the Lyα emission. The transmission spectrum (assuming an intrinsic power-law continuum[24] of $F_\lambda \propto \lambda^{-1.5}$, where F_λ is the flux density at wavelength λ) is shown in Fig. 2. Complete Gunn–Peterson absorption can also be seen in the Lyα, Lyβ and Lyγ transitions. Statistically significant transmission peaks are detected at $z = 5.99$ in both the Lyα and Lyβ troughs, and an additional transmission peak is detected at $z = 5.84$ in the Lyβ trough. The 2σ lower limit on the Lyα Gunn–Peterson optical depth (τ_α) at $z = 6.00$–6.15 is $\tau_\alpha > 5.5$ and the 2σ lower limit for Lyβ is $\tau_\beta > 6$, corresponding to an equivalent $\tau_\alpha > 13.5$, following the conversion in literature[16]. The characteristics of the intergalactic medium (IGM) transmission along the line of sight of J0100+2802, including the deep Lyα and Lyβ troughs, and the narrow, unresolved transmission peaks, are similar to those observed in SDSS J1148+5251, and are consistent with the rapid increase in the IGM neutral fraction at $z > 5.5$ observed in a large sample of SDSS quasars[16]. The size evolution of the quasar proximity zone, which is highly ionized by quasar ultraviolet photons, can also be used to constrain the IGM neutral fraction. The size of the proximity zone is defined by the point where the transmitted flux first drops by a significant amount to below 10% (ignoring small absorption leaks) of the quasar extrapolated continuum emission after the spectrum is smoothed to a resolution of 20 Å (ref. 16). As shown in Fig. 2, J0100+2802 has a much larger proper proximity zone (7.9 ± 0.8 Mpc; 1 Mpc is about 3.26 million light years) than that of other SDSS quasars[16,25] at $z > 6.1$; its large proximity zone size is expected from the higher level of photo-ionization dominated by quasar radiation.

We obtained the near-infrared J,H,K-band spectra with Gemini and Magellan telescopes on 6 August and 7 October 2014, respectively (see Methods for details). Figure 3 shows the combined optical/near-infrared spectrum of J0100+2802 and the results of fitting the Mg II emission line. The Mg II full-width at half-maximum (FWHM) is 5,130 ± 150 km s^{-1}, and the continuum luminosity at the rest-frame wavelength of 3,000 Å is $(3.15 \pm 0.47) \times 10^{47}$ erg s^{-1}. After applying a virial black-hole mass estimator based on the Mg II line[26], we estimate its black-hole mass to be $(1.24 \pm 0.19) \times 10^{10}\, M_\odot$. The uncertainty of black-hole mass does not include the systematic uncertainty of virial black-hole mass estimation, which could be up to a factor of three[27]. Assuming that this quasar is accreting at the Eddington accretion rate and the bolometric luminosity is close to the Eddington luminosity ($L_{\rm Edd} = 1.3 \times 10^{38}$ $(M/M_\odot)$), similar to other $z > 6$ quasars[11], leads to a black-hole mass of

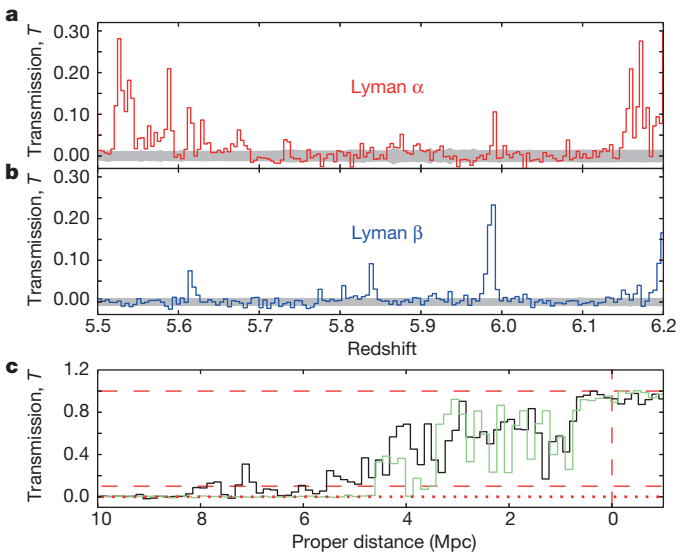

Figure 2 | Transmission in absorption troughs and the proximity zone for J0100+2802. **a**, **b**, Transmission in Lyα and Lyβ absorption troughs (respectively **a**, red; **b**, blue) were calculated by dividing the spectrum by a power-law continuum[24], $F_\lambda \propto \lambda^{-1.5}$. The shaded band in both panels shows 1σ standard deviation. The Lyα and Lyβ absorption redshifts are given by $\lambda/\lambda_{\rm Lyα(Lyβ)} - 1$, where $\lambda_{\rm Lyα} = 1{,}216$ Å and $\lambda_{\rm Lyβ} = 1{,}026$ Å. The optical spectrum exhibits a deep Gunn–Peterson trough and a significant transmission peak at $z = 5.99$. **c**, Transmission in the proximity zone. The proper proximity zone for J0100+2802 (in black) extends to 7.9 ± 0.8 Mpc, a much larger value than those of other $z > 6.1$ quasars, including 4.9 ± 0.6 Mpc for J1148+5251 (in green), consistent with its higher ultraviolet luminosity. The transmission in **c** was calculated by dividing the measured spectrum by a power-law continuum $F_\lambda \propto \lambda^{-1.5}$ plus two Gaussian fittings of Lyα and N v lines. The horizontal dotted line and the two dashed lines denote transmission values of 0, 0.1 and 1.0 respectively, while the vertical dashed line denotes the proper proximity zone size of 0.

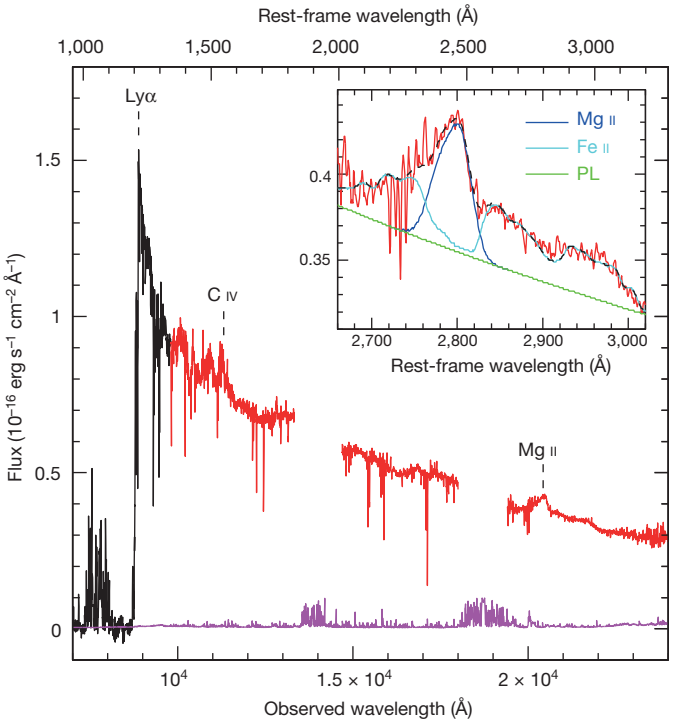

Figure 3 | The combined optical/near-infrared spectrum of J0100+2802 and the fitting of the Mg II line. Main panel, the black line shows the LBT optical spectrum and the red line shows the combined Magellan and Gemini near-infrared J,H,K-band spectra (from left to right, respectively). The gaps between J and H and between H and K bands are ignored due to the low sky transparency there. The magenta line shows the noise spectrum. The main emission lines Lyα, C IV and Mg II are labelled. The details of the absorption lines are described in Extended Data Fig. 4. Inset, fits of the Mg II line (with FWHM of 5,130 ± 150 km s^{-1}) and surrounding Fe II emissions. The green, cyan and blue solid lines show the power law (PL), Fe II and Mg II components. The black dashed line shows the sum of these components in comparison with the observed spectrum, denoted by the red line. The black-hole mass is estimated to be $(1.24 \pm 0.19) \times 10^{10}\, M_\odot$.

$1.3\times10^{10}M_{\odot}$ for J0100+2802. Therefore, our observations strongly indicate that J0100+2802 harbours a black hole of mass about $1.2\times10^{10}M_{\odot}$, the first such system known at $z>6$, though black holes of such a size have been found in local giant elliptical galaxies[28] and low-redshift quasars[21].

Although gravitational lensing is a possible explanation for the high luminosity of J0100+2802, we do not expect a large lensing magnification. An LBT K-band image with seeing of 0.4″ shows a morphology fully consistent with a single point source (Extended Data Fig. 2); and the large size of the quasar proximity zone further supports a high ultraviolet luminosity consistent with the expected photoionization scaling[29]. However, absorption features at different redshift have been identified from its near-infrared spectroscopy (Extended Data Fig. 4), implying the existence of abundant intervening materials along the line of sight.

J0100+2802 is the only known quasar with a bolometric luminosity higher than 10^{48} erg s^{-1} and a black-hole mass larger than $5\times10^{9}M_{\odot}$ at $z\geq6$. It is also close to being the most luminous quasar with the most massive black hole at any redshift (Fig. 4). The discovery of this single ultraluminous quasar within the entire SDSS footprint (~13,000 degrees[2]) is broadly consistent with the extrapolation of the SDSS $z\approx6$ quasar luminosity function[16]. The number density of such objects would set strong constraints on the early growth of supermassive black holes and the evolution of the high-redshift quasar black-hole mass function[5,11]. In addition to ULAS J1120+0641 with a $2\times10^{9}M_{\odot}$ black hole[6,13] at $z=7.085$, and a recently discovered $z=6.889$ quasar with a black hole of $2.1\times10^{9}M_{\odot}$ (ref. 13), J0100+2802 with a $1.2\times10^{10}M_{\odot}$ black hole at $z=6.30$ presents the next most significant challenge to the Eddington-limited growth of black holes in the early Universe[11,14]. Its existence also strengthens the claim that supermassive black holes in the early Universe probably grew much more quickly than their host galaxies, as argued from a molecular gas study of $z\approx6$ quasars[30]. Therefore, as the most luminous quasar known to date at $z>6$, J0100+2802 will be a unique resource for the future study of mass assembly and galaxy formation around the most massive black holes at the end of the epoch of cosmic reionization[16].

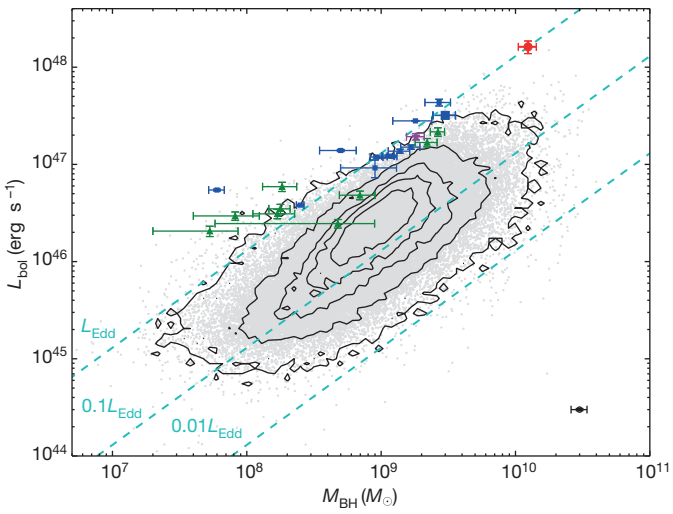

Figure 4 | Distribution of quasar bolometric luminosities, $L_{\rm bol}$, and black-hole masses, $M_{\rm BH}$, estimated from the Mg II lines. The red circle at top right represents J0100+2802. The small blue squares denote SDSS high-redshift quasars[2,10,12], and the large blue square represents J1148+5251. The green triangles denote CFHQS high-redshift quasars[11,12]. The purple star denotes ULAS J1120+0641 at $z=7.085$ (ref. 6). Black contours (which indicate 1σ to 5σ significance from inner to outer) and grey dots denote SDSS low-redshift quasars[21] (with broad absorption line quasars excluded). Error bars represent the 1σ standard deviation, and the mean error bar for low-redshift quasars is presented in the bottom-right corner. The dashed lines denote the luminosity in different fractions of the Eddington luminosity, $L_{\rm Edd}$. Note that the black-hole mass and bolometric luminosity are calculated using the same method and the same cosmology model as in the present Letter, and the systematic uncertainties (not included in the error bars) of virial black-hole masses could be up to a factor of three[27].

Online Content Methods, along with any additional Extended Data display items and Source Data, are available in the online version of the paper; references unique to these sections appear only in the online paper.

Received 17 June 2014; accepted 15 January 2015.

1. Fan, X. *et al.* A survey of $z>5.7$ quasars in the Sloan Digital Sky Survey. II. Discovery of three additional quasars at $z>6$. *Astron. J.* **125,** 1649–1659 (2003).
2. Jiang, L. *et al.* Gemini near-infrared spectroscopy of luminous $z\sim6$ quasars: chemical abundances, black hole masses, and Mg II absorption. *Astron. J.* **134,** 1150–1161 (2007).
3. Willott, C. J. *et al.* Four quasars above redshift 6 discovered by the Canada-France high-z quasar survey. *Astron. J.* **134,** 2435–2450 (2007).
4. Jiang, L. *et al.* A survey of $z\sim6$ quasars in the Sloan Digital Sky Survey deep stripe. I. A flux-limited sample at $z_{AB}<21$. *Astron. J.* **135,** 1057–1066 (2008).
5. Willott, C. J. *et al.* The Canada-France high-z quasar survey: nine new quasars and the luminosity function at redshift 6. *Astron. J.* **139,** 906–918 (2010).
6. Mortlock, D. J. *et al.* A luminous quasar at a redshift of $z=7.085$. *Nature* **474,** 616–619 (2011).
7. Venemans, E. P. *et al.* Discovery of three $z>6.5$ quasars in the VISTA Kilo-Degree Infrared Galaxy (VIKING) Survey. *Astrophys. J.* **779,** 24–36 (2013).
8. Bañados, E. *et al.* Discovery of eight $z\sim6$ quasars from Pan-STARRS. *Astron. J.* **148,** 14–25 (2014).
9. Willott, C. J., McLure, R. J. & Jarvis, M. J. A $3\times10^{9}M_{\odot}$ black hole in the quasar SDSS J1148+5251 at $z=6.41$. *Astrophys. J.* **587,** L15–L18 (2003).
10. Kurk, J. D. *et al.* Black hole masses and enrichment of $z\sim6$ SDSS quasars. *Astrophys. J.* **669,** 32–44 (2007).
11. Willott, C. J. *et al.* Eddington-limited accretion and the black hole mass function at redshift 6. *Astron. J.* **140,** 546–560 (2010).
12. De Rosa, G. *et al.* Evidence for non-evolving Fe II/Mg II ratios in rapidly accreting $z\sim6$ QSOs. *Astrophys. J.* **739,** 56–69 (2011).
13. De Rosa, G. *et al.* Black hole mass estimates and emission-line properties of a sample of redshift $z>6.5$ quasars. *Astrophys. J.* **790,** 145–158 (2014).
14. Volonteri, M. The formation and evolution of massive black holes. *Science* **337,** 544–547 (2012).
15. Gunn, J. E. & Peterson, B. A. On the density of neutral hydrogen in intergalactic space. *Astrophys. J.* **142,** 1633–1641 (1965).
16. Fan, X., Carilli, C. L. & Keating, B. Observational constraints on cosmic reionization. *Annu. Rev. Astron. Astrophys.* **44,** 415–462 (2006).
17. York, D. G. *et al.* The Sloan Digital Sky Survey: technical summary. *Astron. J.* **120,** 1579–1587 (2000).
18. Skrutskie, M. F. *et al.* The Two Micron All Sky Survey (2MASS). *Astron. J.* **131,** 1163–1183 (2006).
19. Wright, E. L. *et al.* The Wide-field Infrared Survey Explorer (WISE): mission description and initial on-orbit performance. *Astron. J.* **140,** 1868–1881 (2010).
20. Wu, X.-B. *et al.* SDSS quasars in the WISE preliminary data release and quasar candidate selection with optical/infrared colours. *Astron. J.* **144,** 49–59 (2012).
21. Shen, Y. *et al.* A catalog of quasar properties from Sloan Digital Sky Survey data release 7. *Astrophys. J.* **194** (suppl.), 45–65 (2011).
22. Fan, X. *et al.* The discovery of a high-redshift quasar without emission lines from Sloan Digital Sky Survey commissioning data. *Astrophys. J.* **526,** L57–L60 (1999).
23. Wang, R. *et al.* Thermal emission from warm dust in the most distant quasars. *Astrophys. J.* **687,** 848–858 (2008).
24. Vanden Berk, D. E. *et al.* Composite quasar spectra from the Sloan Digital Sky Survey. *Astron. J.* **122,** 549–564 (2001).
25. Carilli, C. L. *et al.* Ionization near zones associated with quasars at $z\sim6$. *Astrophys. J.* **714,** 834–839 (2010).
26. McLure, R. J. & Dunlop, J. S. The cosmological evolution of quasar black hole masses. *Mon. Not. R. Astron. Soc.* **352,** 1390–1404 (2004).
27. Peterson, B. M. *et al.* Central masses and broad-line region sizes of active galactic nuclei. II. A homogeneous analysis of a large reverberation-mapping database. *Astrophys. J.* **613,** 682–699 (2004).
28. McConnell, N. J. *et al.* Two ten-billion-solar-mass black holes at the centres of giant elliptical galaxies. *Nature* **480,** 215–218 (2011).
29. Haiman, Z. *et al.* Constraining reionization with the evolution of the luminosity function of Lyα emitting galaxies. *Astron. J.* **623,** 627–631 (2005).
30. Wang, R. *et al.* Molecular gas in $z\sim6$ quasar host galaxies. *Astrophys. J.* **714,** 699–712 (2010).

Supplementary Information is available in the online version of the paper.

Acknowledgements X.-B.W. thanks the NSFC (grant nos 11033001 and 11373008), the Strategic Priority Research Program 'The Emergence of Cosmological Structures' of the Chinese Academy of Sciences (grant no. XDB09000000), and the National Key Basic Research Program of China (grant no. 2014CB845700) for support. X.F., R.W. and I.D.M. thank the US NSF (grant nos AST 08-06861 and AST 11-07682) for support. R.W. thanks the NSFC (grant no. 11443002) for support. We acknowledge the support of the staff of the Lijiang 2.4-m telescope. Funding for the telescope was provided by the Chinese Academy of Sciences and the People's Government of Yunnan Province. This

research uses data obtained through the Telescope Access Program (TAP), which has been funded by the Strategic Priority Research Program 'The Emergence of Cosmological Structures' (grant no. XDB09000000), National Astronomical Observatories, Chinese Academy of Sciences, and the Special Fund for Astronomy from the Ministry of Finance of China. We thank D. Osip for help with Magellan/FIRE spectroscopy, and Y.-L. Ai, L. C. Ho, Y. Shen and J.-G. Wang for suggestions about data analyses. We acknowledge the use of SDSS, 2MASS and WISE data, and of the MMT, LBT, Gemini and Magellan telescopes; detailed acknowledgments of these facilities can be found in Supplementary Information.

Author Contributions X.-B.W., F.W. and X.F. planned the study, and wrote the draft version of the paper. All other co-authors contributed extensively and equally to the observations, data analyses and writing of the manuscript.

Author Information Reprints and permissions information is available at www.nature.com/reprints. The authors declare no competing financial interests. Readers are welcome to comment on the online version of the paper. Correspondence and requests for materials should be addressed to X.-B.W. (wuxb@pku.edu.cn).

METHODS

The optical spectroscopy on J0100+2802 was first carried out on 29 December 2013 with the Yunnan Fainter Object Spectrograph and Camera (YFOSC) of the Lijiang 2.4-m telescope in China. We used a very low resolution grism (G12, at a dispersion of 18 Å per pixel) and took 3,000 s exposure on this target. The spectrum clearly shows a sharp break at about 8,800 Å and no significant emissions blueward, consistent with a quasar spectrum at a redshift beyond 6.2. To confirm this discovery, two subsequent optical spectroscopic observations were obtained on 9 and 24 January 2014 with the 6.5-m Multiple Mirror Telescope (MMT) and the twin 8.4-m mirror Large Binocular Telescope (LBT) in the USA, respectively. The low to medium resolution spectra, obtained with 1,200 s exposure using the MMT Red Channel (at a dispersion of 3.6 Å per pixel) and 2,400 s exposure with the LBT Multi-Object Double CCD Spectrographs/Imagers (MODS)[31] (at a dispersion of 1.8 Å per pixel) respectively, explicitly confirm that SDSS J0100+2802 is a quasar at redshift 6.30 ± 0.01 (obtained by the Lyα line).

The near-infrared K-band spectroscopy on J0100+2802 was carried out with LBT/LUCI-1 on 2 January 2014. Owing to the short exposure time (15 min), the spectrum is of modest signal-to-noise ratio (*S*/*N*). Although the Mg II line was clearly detected, the noisy LBT spectrum did not allow us to accurately measure the line width. To improve the quality of the near-infrared spectrum, we obtained J,H,K-band spectroscopy with Gemini/GNIRS and Magellan/FIRE on 6 August and 7 October 2014, respectively. The exposure time was 3,600 s for GNIRS and 3,635 s for FIRE. The FIRE spectrum has higher *S*/*N* (about 30 in K band) and higher spectral resolution ($R = \lambda/\Delta\lambda \approx 6{,}000$) than the GNIRS spectrum (with *S*/*N* of about 10 in K band and $R \approx 1{,}800$). In order to achieve the best spectral quality, we combined the FIRE and the GNIRS spectra, and scaled the combined spectrum according to its 2MASS J,H,K_s-band magnitudes. The Mg II line shown in the K-band spectrum gives the same redshift as that given by the Lyα line in the optical spectrum. The high-quality J,H,K-band spectra also clearly display abundant absorption features, which have been identified as being from intervening or associated systems with redshifts from 2.33 to 6.14 (Extended Data Fig. 4).

After redshift and Galactic extinction corrections, the rest-frame H- and K-band spectrum is decomposed into a pseudo-continuum and the Mg II emission line. The pseudo-continuum consists of a power-law continuum and Fe II emissions, and is fitted within the rest-frame wavelength range between 2,000 Å and 3,200 Å by excluding the boundary region between H and K bands where the sky transparency is lower. An Fe II template[32,33] is adopted for the fitting of Fe II emissions. The Mg II emission line is fitted with two broad Gaussian components. The four Mg II absorption lines near the redder part of the Mg II emission line are also fitted as four Gaussian lines in order to remove their effects on the fittings of Mg II and Fe II emission lines. The overall FWHM of the Mg II emission line is ~5,130 km s^{-1} with an uncertainty of 150 km s^{-1}. The continuum has a slope of −1.43 and the continuum luminosity at the rest-frame wavelength of 3,000 Å ($L_{3,000}$) is $(3.15 \pm 0.47) \times 10^{47}$ erg s^{-1}. The Fe II to Mg II line ratio is 2.56 ± 0.18, which is consistent with the mean value of other $z > 6$ quasars[12,13]. After applying a virial black-hole mass estimator based on the Mg II line[26], we estimate its black-hole mass to be $(1.24 \pm 0.19) \times 10^{10}\ M_{\odot}$. Although the systematic uncertainty of virial black-hole mass estimation can be up a factor of three[27], our result still strongly indicates that J0100+2802 hosts a central black hole with mass close to $1.2 \times 10^{10}\ M_{\odot}$. This is also well consistent with a black-hole mass obtained by assuming an Eddington luminosity of J0100+2802, which leads to a mass of $1.3 \times 10^{10}\ M_{\odot}$. Considering the contribution of Balmer continuum, as done for other $z > 6$ quasars[12,13], leads to a decrease of $L_{3,000}$ to $(2.90 \pm 0.44) \times 10^{47}$ erg s^{-1}, an increase of FWHM of Mg II to $5{,}300 \pm 200$ km s^{-1} and yields a black-hole mass of $(1.26 \pm 0.21) \times 10^{10}\ M_{\odot}$. Therefore, the effect of considering Balmer continuum is insignificant for the black-hole mass measurement of J0100+2802. In addition, if we adopt a different virial black-hole mass scaling relation[34], the black-hole mass changes to $(1.07 \pm 0.14) \times 10^{10}\ M_{\odot}$, which is still well consistent with the result we obtained above.

Sample size. No statistical methods were used to predetermine sample size.

31. Pogge, R. W. *et al.* The multi-object double spectrographs for the Large Binocular Telescope. *Proc. SPIE* **7735,** 9–16 (2010).
32. Vestergaard, M. & Wilkes, B. J. An empirical ultraviolet template for iron emission in quasars as derived from I Zwicky 1. *Astrophys. J. Suppl. Ser.* **134,** 1–33 (2001).
33. Salviander, S. *et al.* The black hole mass-galaxy bulge relationship for QSOs in the Sloan Digital Sky Survey data release 3. *Astrophys. J.* **662,** 131–144 (2007).
34. Vestergaard, M. & Osmer, P. S. Mass functions of the active black holes in distant quasars from the Large Bright Quasar Survey, the Bright Quasar Survey, and the color-selected sample of the SDSS Fall Equatorial Stripe. *Astrophys. J.* **699,** 800–816 (2009).

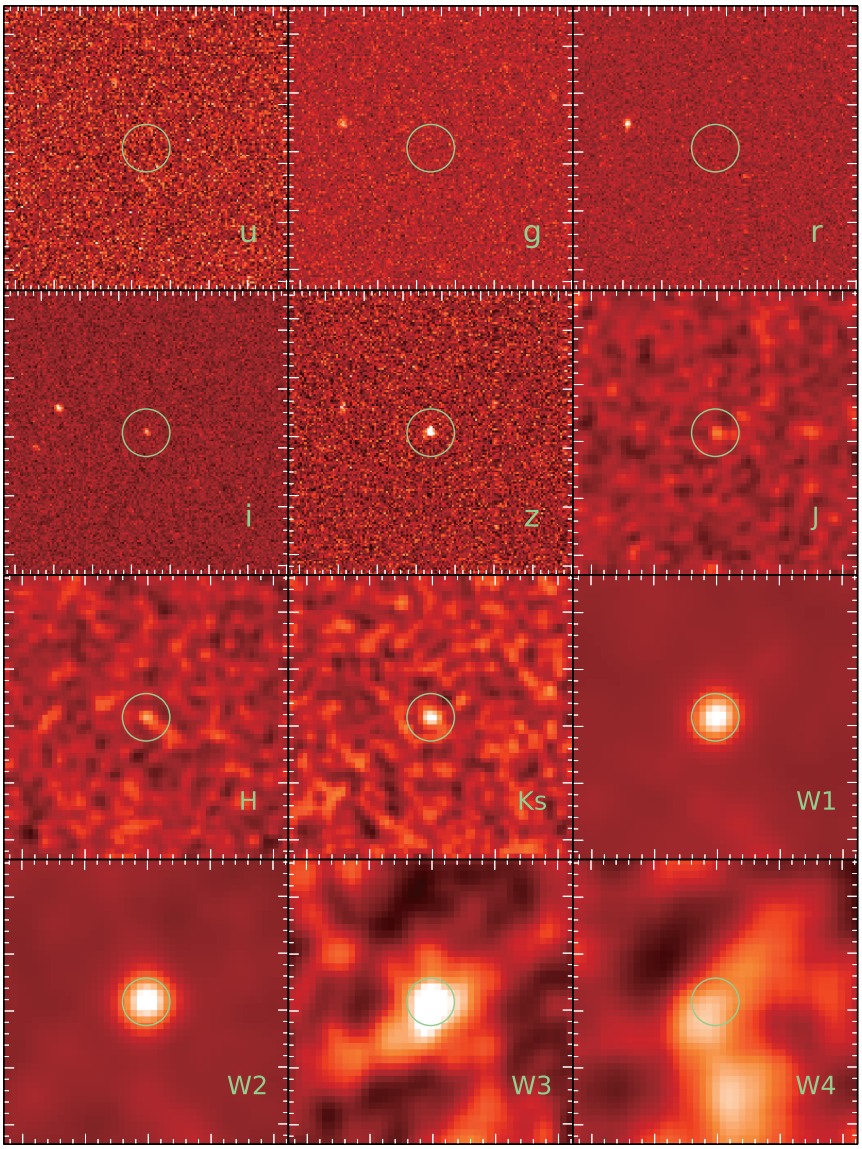

Extended Data Figure 1 | Images of J0100+2802 in SDSS, 2MASS and WISE bands. J0100+2802 is undetected in SDSS u,g,r bands (top row) but is relatively bright in other bands (lower three rows). It is consistent with a point source in the bands with high signal-to-noise detections. The size is $1' \times 1'$ for all images. The green circle represents an angular size of 10″ in each image.

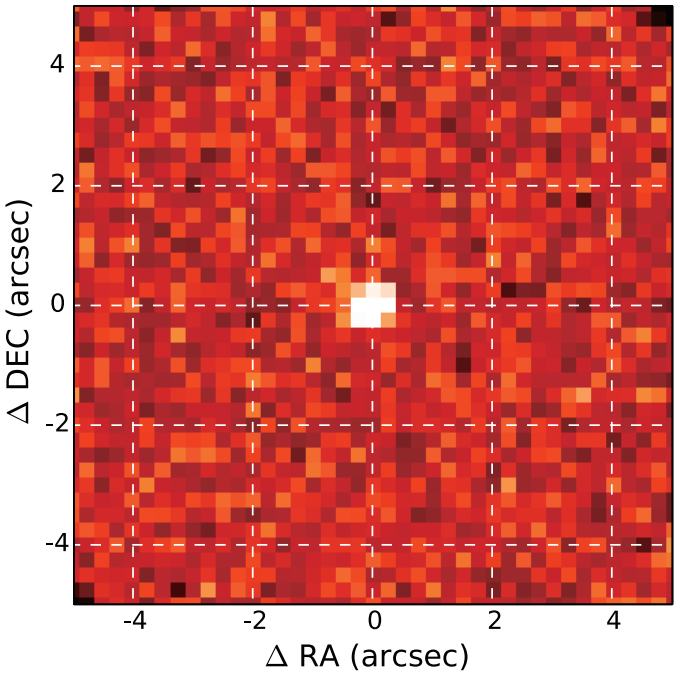

Extended Data Figure 2 | The LBT K-band image of J0100+2802. The size is 10″ × 10″. The horizontal and vertical axes denote the offsets in right ascension (ΔRA) and in declination (ΔDec.). The image, with seeing of 0.4″, shows a morphology fully consistent with a point source.

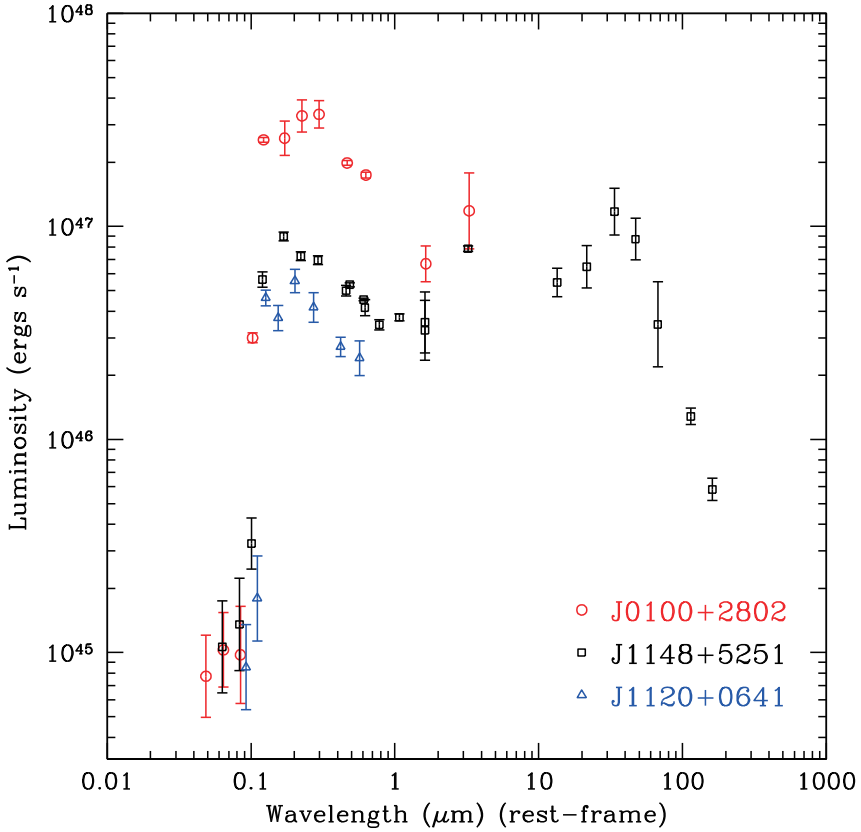

Extended Data Figure 3 | The rest-frame spectral energy distributions of J0100+2802, J1148+5251 and ULAS J1120+0641. The redshifts of these three quasars are 6.30, 6.42 and 7.085, respectively. The luminosity of J0100+2802 in the ultraviolet/optical bands is about four times higher than that of J1148+5251, and seven times higher than that of ULAS J1120+0641. The photometric data are from literature for J1148+5251 and J1120+0641. The error bars show the 1σ standard deviation.

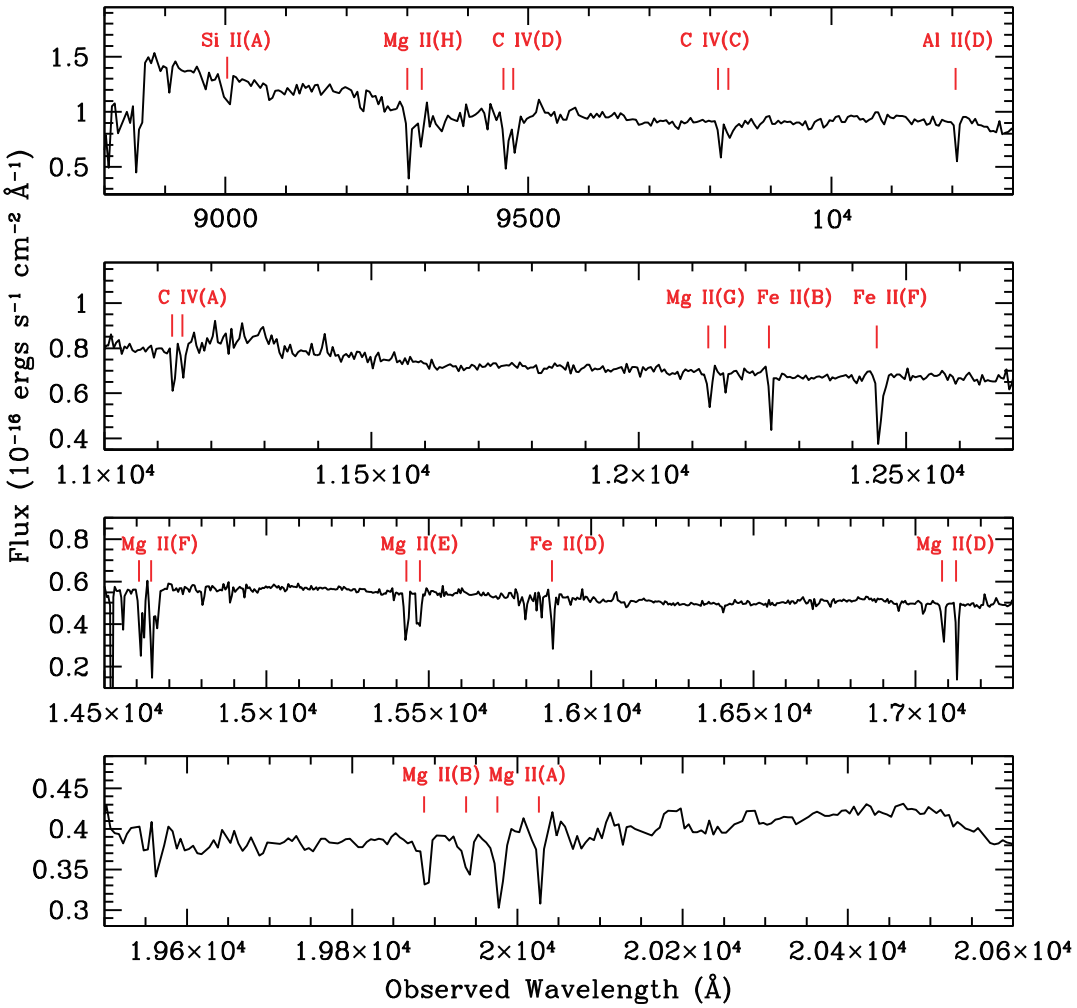

Extended Data Figure 4 | The major absorption features identified from optical and near-infrared spectroscopy of J0100+2802. Most of them are from Mg II, C IV and Fe II. The labels from A to H correspond to the redshifts of absorption materials at 6.14, 6.11, 5.32, 5.11, 4.52, 4.22, 3.34 and 2.33, respectively. Studies of intervening and associated absorption systems will be discussed elsewhere.